Available online at www.eccomasproceedia.org
Eccomas Proceedia SMART (2023) 850-865

ECCOMAS
Proceedia

X ECCOMAS Thematic Conference on Smart Structures and Materials
SMART 2023
D.A. Saravanos, A. Benjeddou, N. Chrysochoidis and T. Theodosiou (Eds)

OPERATIONAL EXPERIENCE DURING A FOUR YEAR TEST PROGRAM OF ACTIVE FLAPS ON A WIND TURBINE BLADE

ALEJANDRO GOMEZ GONZALEZ*, PEDER B. ENEVOLDSEN*, ANDREA GAMBERINI*†, ATHANASIOS BARLAS† AND HELGE AA. MADSEN†

*Siemens Gamesa Renewable Energy A/S (SGRE)
Technology Development
Borupvej 16, 7330 Brande, Denmark
e-mail: alejandro.gonzalez@siemensgamesa.com, web page: http://www.siemensgamesa.com/

† DTU Wind and Energy Systems (DTU Wind)
DTU Risø Campus
Frederiksborgvej 399, 4000 Roskilde, Denmark
Web page: http://wind.dtu.dk

Abstract. A prototype of a pneumatically controlled active flap system (AFS) for wind turbine blades was designed and manufactured as a part of the collaboration projects Induflap2 and VIAs between the partners Siemens Gamesa Renewable Energy, DTU Wind, and Rehau. The AFS was validated in full-scale during a four year test program consisting of four individual test phases between 2018 and 2022 on two different test turbines with rated powers of 4.0 and 4.3 MW, respectively. The objective of the field validation was to collect operational experience with the complete system, to perform a detailed experimental aerodynamic and aeroelastic characterization of the wind turbine equipped with an AFS, and to validate the numerical models used for the simulation of such a system. Besides the validation activities, different experimental techniques were developed in order to enable the accurate measurement of aerodynamic quantities within a highly dynamic and turbulent wind environment. The load control authority of the AFS was measured to be in the range of 3-20% for the flapwise bending moment. Very good agreement was found when compared to aeroelastic simulations. Furthermore, a direct measurement of fatigue reduction on the blades was performed employing a cyclic approach for the flap control leading to load reductions in the range of 10-13%. This paper discusses the main results of the complete four-year test program based on the load measurements and operational experience collected.

Key words: Wind Turbines, Smart Blades, Active Flow Control, Active Flaps, Field Tests

1 INTRODUCTION

The development of new wind turbines is continuously pushing the limits of current technology fronts within the fields of aeroelasticity, structural mechanics, material science, and

Peer-review under responsibility of the organizing committee of SMART 2023.
doi: 10.7712/150123.9838.444885

advanced control, among others. With time, the design drivers of wind turbine blades have changed significantly with the demand for longer flexible blades. Blade design drivers can be related for example to extreme material strains, maximum allowable tip deflection, blade-hub interface loading, or stability limits of blades. The ability to tailor the aerodynamic performance of blades has continuously evolved, beginning with fixed pitch passive stall controlled in the late 1970's, active stall fixed-speed controlled turbines during the 1980's and 1990's, and a transition to pitch-to-feather variable-speed controlled turbines in the early 1990's and going forward. Additional degrees of aerodynamic and aeroelastic tailoring were introduced at industrial level towards the end of the 2000's and beginning of 2010's with the increased use of passive aerodynamic add-ons such as vortex generators and trailing edge serrations, as well as aeroelastic tailoring by means of bend twist coupling of the blades. An even higher degree of control authority on the aerodynamic loads introduced to the turbine and the foundation can be achieved by implementing active flow control techniques such as trailing edge flaps.

The two research projects Induflap2 (2015-2018) and VIAs (2019-2022) carried out by the partners SGRE, DTU Wind, and Rehau, aimed at developing a system of active trailing edge flaps suitable for industrial application and to demonstrate the technology in full-scale on modern wind turbines. During these two projects, a series of design iterations of the active flap were carried out, each tested at different levels of fidelity (wind tunnel, lab scale, rotating test rig, or full-scale as shown schematically in figure 1). The full-scale testing of the active flap system (AFS) was performed in four phases during which some upgrades were performed to the system based both on the operational experience collected as well as on results from laboratory and wind tunnel testing performed in parallel to the field test. This article collects some selected findings and learnings during the four-year test program and guides the reader to further references wherever applicable.

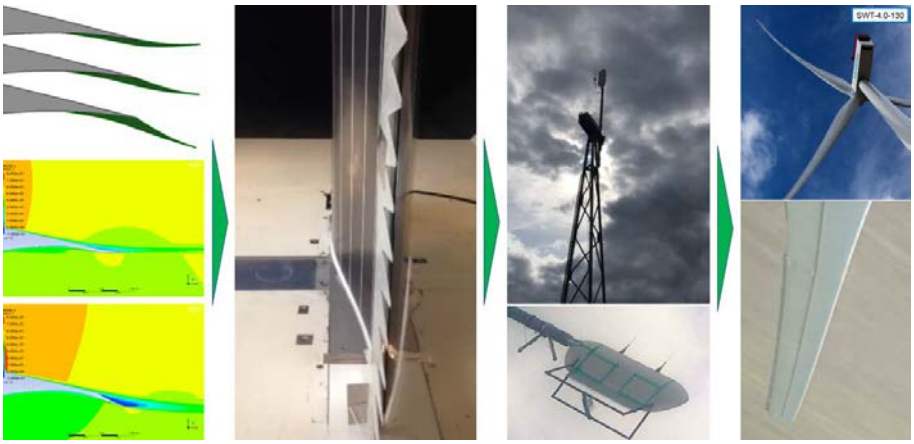

Figure 1: Schematic representation of validation steps of the active flap system, starting from detailed design activities such as CFD, proceeding with sub-system tests at wind tunnel and rotating test rig level, and concluding with full-scale verification

The article is structured as follows. The first section describes briefly the objectives of the two aforementioned publicly funded projects Induflap2 and VIAs. The next section gives a brief description of the state of the art in the field of flow control, with focus on the field validation activities. The following two sections discuss the test setup, the methodology, and results of the field validation of the AFS. These sections focus mainly on three specific validation exercises carried out: the validation of the load control authority of the active flap by means of the so-called blade-2-blade method, detailed aerodynamic measurements based on advanced inflow and pressure sensors, and detailed aeroelastic characterization by means of so-called one-2-one aeroelastic simulations. The last section summarizes the work in the form of conclusions and lessons learned.

2 OBJECTIVE

The main objective of the Induflap2 and VIAs[1] projects was to design, manufacture, and validate an AFS for rotor blades of wind turbines at different fidelity scales, as well as to develop the necessary experimental and numerical methods. The validation of the active flow control systems is not only complex, but also costly. Therefore, for these two projects to be successful, a good collaboration between industry and academic partners has proven essential. Secondary objectives of the project include

- the structural, aerodynamic, and aeroelastic characterization of the isolated AFS at laboratory level (i.e. structural static and fatigue testing, wind tunnel testing, and testing in atmospheric conditions on a rotating test rig)
- the numerical description of the isolated AFS (i.e. FEM, CFD, and FSI simulations), as well as the numerical evaluation of the full wind turbine and AFS assembly by means of aeroelastic simulations
- the development of necessary measurement devices and methods to carry out the aforementioned numerical and experimental tasks
- the demonstration of AFS manufacturing at industrial level
- to identify all the system boundaries of the AFS and mature the required peripheral systems and preliminary control strategies
- to identify technical risks and tackle them in a systematic manner by means of DFMEA's (Design Failure Mode and Effect Analysis)
- to demonstrate the functionality of the system in a long term full-scale test on a modern wind turbine and carry out the required detailed testing and simulation activities relevant to this.

[1]Induflap2 and VIAs were partially funded by EUDP under Journal Nrs. 64015-0069 and 64019-0061, respectively

This article focuses on the last bullet point. To the author's knowledge, the tests carried out during this test program represent the largest (both in terms of rotor diameter as well as rated power of the turbine) and longest (in terms of actual test time at full-scale) in the world up to date.

3 STATE OF THE ART

Reducing the levelized cost of energy (LCOE) of wind turbines can be achieved by increasing the swept area of the rotor while minimizing the loads imposed on the main components such as the hub, nacelle, tower structure, and foundation. An effective way to achieve this is through active flow control. Several active flow control concepts, including active gurney flaps, mini-tabs, plasma actuators, and boundary layer suction and blowing have been studied, but many of these are not suitable for industrial deployment due to technical feasibility and implementation challenges. An overview of some of the main flow control approaches can be found e.g. in [1, 2, 3, 4]. Some of these strategies aim directly at improving the aerodynamic efficiency of a rotor e.g. by suppressing local flow separation. Such concepts are closely related to the field of boundary layer control and include e.g. plasma actuators [5, 6] or boundary layer suction and blowing (also including synthetic jets) [7, 8, 9, 10, 11]. Other concepts focus on circulation control, including e.g. active gurney flaps and mini-tabs [12, 13]. One concept for circulation control is the rigid or morphing trailing edge flap. Such flaps have been the subject of numerous studies in the past, covering both the aerodynamic, structural, and aeroelastic modelling of the turbine-flap system, as well as the development of control strategies for load reduction (see e.g. [14, 15, 16, 17, 18].

Full-scale experimental validation of active flow control strategies is complex and costly. As a consequence, the amount of literature available for full-scale tests (on MW-sized turbines) is scarce. Among the few efforts to do this type of validation, some of the most representative are mentioned here. One representative tests was performed on a Vestas wind turbine type V27-225 kW (13m long blade) equipped with a 70cm long trailing edge flap [19, 20, 17, 18]. In these tests, the AFS was mainly operated in intervals of two minutes with and without flap control focusing mainly on alleviating blade fatigue loads. A further active flap test was carried out by Sandia Laboratories [15, 16] where a mechanically actuated hinged flap covering the aft 20% of the chord of the outer 20% span of a 9m long blade was tested. Previous work on morphing flaps carried out within the framework of the Induflap1 project [21] includes testing under atmospheric conditions in the rotating test rig as well [22, 23]. During these tests, measurements of the flapwise bending moment of the boom of the rotating rig show that a 5 deg flap actuation (15% chordwise coverage) has a similar response as 1 deg blade section pitch actuation. Similar tests were performed on a morphing trailing edge flap [14, 24, 25] developed within the framework of the EU INNWind project and was tested under atmospheric conditions on a rotating test rig at the Risoe Campus of DTU. These tests included flap actuation steps, cyclic control based on azimuth position and feed-forward control based on inflow angle. For different blade pitch positions, the AFS was actuated in cycles of 10s over a test period of 5 minutes. Azimuth and inflow based feed forward control showed an average reduction of the standard deviation

of the bending moment at the base of the rotating rig boom of 12% and 11%, respectively. Besides circulation control tests (flaps), a full-scale test of a boundary layer control system with leading edge plasma actuators was performed on a 1.75 MW wind turbine [6]. Swap intervals of 10 minutes (plasma actuators on or off) were performed focusing on the turbine's power production.

The work presented in this article contributes to the state of the art by extending previously reported results of laboratory and full-scale validation of the AFS described in [26, 27, 28] to include test phase 4, and by collecting important lessons learned of complete field validation program. The test setup, instrumentation, methodology, and results are discussed in what follows.

4 TEST SETUP AND TURBINE INSTRUMENTATION

The AFS was tested on two turbines of types SWT-4.0-130 (4.0MW rated power, 130m rotor diameter) and SG-4.3-120 DD (4.3MW rated power, 120m rotor diameter) for a total of four years. The full-scale validation campaign served as basis for the three validation exercises presented in this article: full scale aeroelastic validation via load measurements on the turbine, detailed aerodynamic measurements with help of advanced inflow and pressure blade instrumentation, and validation of aeroelastic models of the turbine including AFS in the codes HAWC2 [29] and BHawC [30, 31].

The field validation of the AFS was carried out in four phases as summarized in table 1. The test program was carried out in the test site Høvsøre in northwest Denmark. The test site layout is shown in figure 2. In all phases of testing, the test turbines were equipped with numerous sensors including strain gauges at the root of the blades (installed at 1.2m from the root for test phase 1 and 2, and 3.0m from the root for test phase 3 and 4) to measure flapwise and edgewise bending moments, acceleration measurements in the nacelle, as well as all operation parameters of the wind turbines including nacelle wind speed, rotor speed, pitch position, electrical power, yaw position, and azimuth position, among others. Furthermore, the wind field was measured employing the combination of a meteorological mast[2] (met-mast) and a Lidar. The met-masts were located at a distance of 2.5 rotor diameters upstream in the westerly sector for each turbine and were used to acquire hub-height wind speed, turbulence level, pressure, temperature, and humidity. The Lidar measured wind speed and direction at ten independent heights spanning the full swept area of the rotor[3]. A complete description of the test setup is given in [26, 27] and shown schematically in figure 3.

Each testing phase was carried out aiming at collecting test data for a wide range of operational conditions of the turbine. As an example, the frequency distribution of wind speed and turbulence intensity at hub-height for test phase 3 is shown in figure 4 covering the full operational range of the wind turbine up to wind speeds beyond 25 m/s.

[2]For phase 3, the met-mast was only available until February 2021

[3]The Lidar is next to the met-mast used during phase 1 and 2 - see figure 2 and was only used to collect wind shear data

	Phase 1	**Phase 2**
Date	Oct 2017 - June 2018	Dec 2018 - June 2019
Turbine	SWT-4.0-130	SWT-4.0-130
AFS revision	FT008rev9	FT008rev10
AFS actuation	discretely adjustable	continuously adjustable
Validation type	on-off cycles	on-off cycles
Location on blade	47.5 - 62.5 m	42.5 - 62.5 m
Other tests	Flow visualization	None
	Phase 3	**Phase 4**
Date	June 2020 - June 2021	July 2021 - Aug 2022
Turbine	SG-4.3-120 DD	SG-4.3-120 DD
AFS revision	FT008rev10	FT008rev10
AFS actuation	continuously adjustable	continuously adjustable (faster)
Validation type	on-off cycles, cyclic 1P	on-off cycles, cyclic 1P
Location on blade	38.0 - 58.0 m	38.0 - 58.0 m
Other tests	Inflow sensor and pressure belt	Inflow sensor, pressure belt, and wake-rake

Table 1: Campaign information

5 METHODOLOGY AND RESULTS

The following sections give a short description of three main types of validation methods used for assessing the aerodynamic and aeroelastic performance of the wind turbine including the AFS: full scale validation by means of the so-called blade-2-blade method, detailed aerodynamic measurements based on inflow and airfoil pressure measurements, and aeroelastic validation by means of so-called one-2-one simulations.

5.1 Blade-2-blade method

The blade-2-blade (b2b) analysis method aims at isolating the impact of a flow control device (in this case an AFS) on the loading of a rotor blade. A description of part of the method is given in [26]. The method is particularly useful in atmospheric environments where the levels of variation of the operational point of the turbine vary continuously due to atmospheric turbulence. The method mainly consists of three types of analysis: steady state impact, transient response, and impact of damage equivalent loading (fatigue) of the AFS. The b2b method can be used to measure the characteristics of an AFS, in particular its steady-state and transient step response, as well as its response to 1P (once per revolution) cyclic activation. Details of the method for steady-state and transient analysis can be found in [26], and a short extension of the method to include 1P cyclic activation for characterization of damage equivalent (fatigue) loads is given in [28].

The steady state analysis requires a rotor equipped with strain gauges for measuring strains (and indirectly bending moments). One blade of the rotor is equipped with the AFS and is

Figure 2: Test site layout - map data taken from Google Maps (c)

referenced to a neighbour blade without the active system. A typical measurement of flapwise root bending moment as a function of wind speed (in the westerly sector where the met-mast is undisturbed and in front of the turbine) is shown in figure 5 for the reference blade A and the blade equipped with the AFS blade B. Each point in this graph represents the average values of a 10-minute measurement interval. The level of scatter shown is typical for such a load measurement as a function of wind speed. The amount of scatter is partly due to atmospheric turbulence and partly to the coherence level between the undisturbed wind measured at the met-mast and the turbine response (the further away the met-mast is located, the lesser it will be influenced by the presence of the turbine, but the level of coherence between met-mast wind signals and turbine load and power signals becomes worse). It can also be seen that blade B (with the AFS), shows different levels of bending moment, even though it is difficult to discern clearly different loading bands. A clear advantage of the b2b method is seen when plotting the bending moment values of each blade against each other as shown exemplary in figure 6, giving a much better correlation and lower scatter. The reason for this is the high correlation of loads seen by two neighbour blades (because they both experience the same level of azimuthal load variation).

The details of the transient analysis and damage equivalent blade-2-blade analysis are not discussed in this paper and the reader is referred to [27, 28].

Some of the main results of the field validation are described below for phase 3 and 4 of the test campaign. During parts of the test campaing, the AFS was activated in an on-off manner, maintaining the flap position constant during an interval of 10-minutes and subsequently fully deactivating the flap for another 10-minutes. The interval of 10 minutes was chosen as it is standard for many other wind turbine measurements such as power (a 10-minute interval is a good compromise between including sufficient turbulent variations but excluding wind speed trend variations and is a standard measurement interval in the industry). The AFS is activated

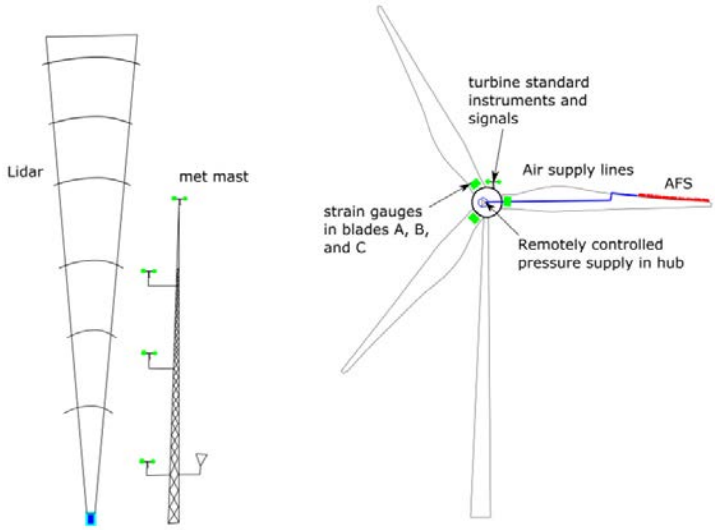

Figure 3: Schematic representation of instrumentation setup

in five discrete states, labelled 0%, 25%, 50%, 75%, and 100%. The lowest and highest activation states correspond to active flap angular deflections of approximately 0 deg and 23 deg (as described in [28], respectively. These on-off activations were performed during several months, collecting data for all activation ranges of the AFS, even though most data was collected for the 75% activation level. The data for the steady state b2b analysis for the AFS is filtered according to low and high wind speeds, for measured hub-height wind speed of less or more than 10 m/s, respectively. This level corresponds approximately with the peak of the load distribution as shown in figure 5 and makes the analysis clearer (the blades operate in quite different aerodynamic conditions before and beyond the peak of bending moment).

The load control authority of the AFS for the different activation states is shown in figure 6 in a b2b manner, and in figure 7 in a relative manner (relative to blade A, without the AFS) as

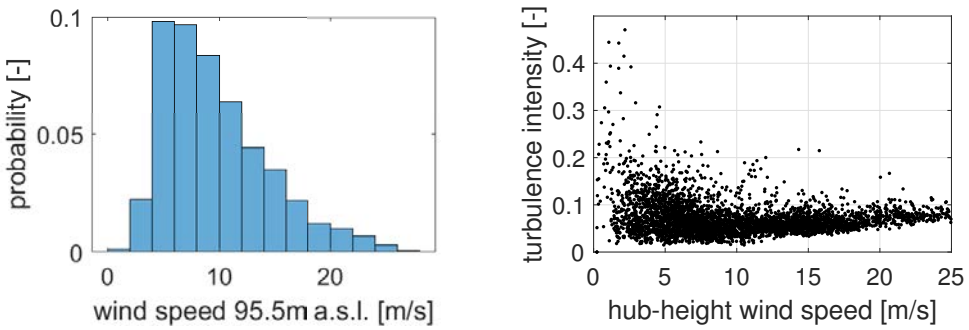

(a) Wind distribution during test phase 3

(b) Turbulence intensity - west sector

Figure 4: Wind conditions during test phase 3

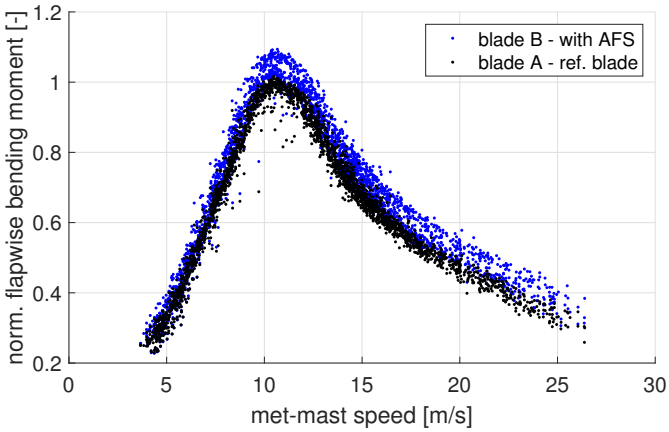

Figure 5: Flapwise bending moment as a function of wind speed measured at the met-mast for phase 3

a function of nacelle wind speed (i.e. the wind speed measured with the nacelle anemometer of the turbine). The steady-state load control authority is seen to range from 3% to 20% depending on the activation state of the flap.

In a further series of tests, the AFS was activated in a feed-forward manner using the azimuth position of the rotor as control signal. The aim of this control strategy was to reduce load variations induced by standard wind shear (i.e. increasing wind speed with increasing height). This simple cyclic approach is a good proxy for the load control authority of the AFS in cyclic conditions. More advanced control strategies are required in order to counteract load imbalance as would occur e.g. from operation in half-wake situations. The reduction in azimuthal load variation of the blades is measured directly by estimating the so-called short term equivalent loads (STEL), which is nothing else than the 1-Hz equivalent load that causes the same amount of damage for a particular Wöhler exponent as the load signal acquired during 10 minutes.

The damage equivalent loads are depicted in figure 8. In this case, for this cyclic 1P feed-forward test periods, the load reduction level measured is approx 10-13% in the range of wind speeds around 12 m/s. The amount of data collected at high wind speeds (higher than approx. 15m/s) is limited.

5.2 Local aerodynamic measurements

Local aerodynamic measurements were performed in a specialized campaign carried out in June 2021 and are reported in [32]. During this campaign, an inflow sensor consisting of a 5-hole Pitot tube and a blade-mounted autonomous data acquisition and transmission system was installed in blade B (including the AFS) in a section in the middle (spanwise) of the AFS extension corresponding to a blade spanwise position of 50m from the hub flange. Furthermore, a pressure belt with 15 taps was installed wrapping around the blade at a spanwise position of 49m. The setup is shown in figure 9a.

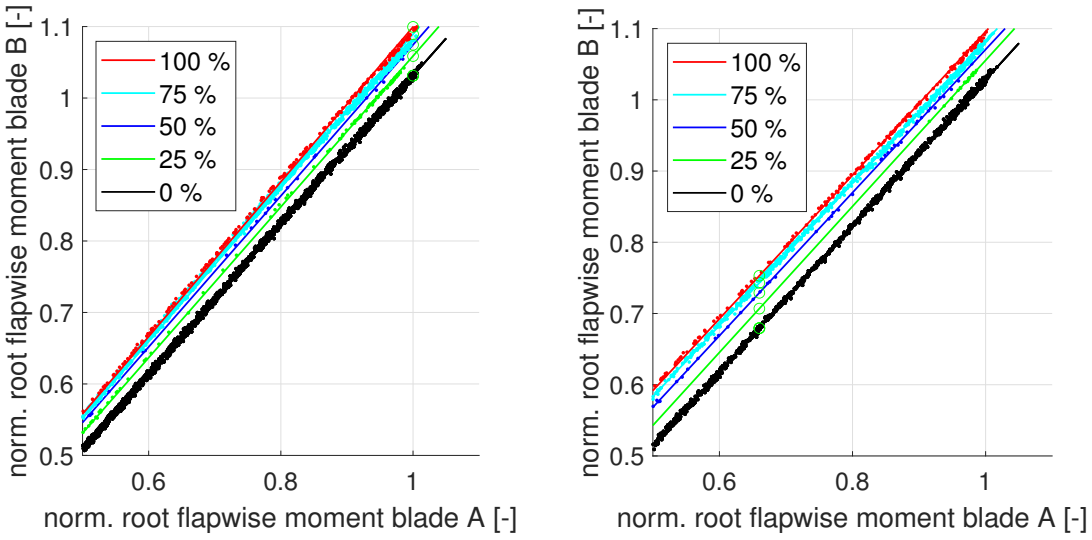

(a) Low wind (b) High wind

Figure 6: Blade-2-blade results during test phase 3 and 4

The tests performed consisted in AFS discrete activations at different flap deflection levels (corresponding to the same activation levels as previously described in the b2b method) and different intervals ranging from 3s to 60s. In parallel to the data acquired by the inflow sensor and pressure belt, all operational characteristics of the turbine as well as the same load channels as described in the previous section were recorded. For visual analysis, a GoPro camera was installed to enable the evaluation of the flap deflection directly from video post-processing and to correlate this with the data acquired from the different instruments.

An exemplary pressure distribution assembled using data from the inflow sensor and the pressure belt is shown in figure 9b for binned data sets of the flap actuated at 0% and 75% levels. The resolution of the position of the taps is enough to identify the main characteristics of the pressure distribution of the airfoil, but has been improved in a more recent experiment with a pressure belt with 32 taps with increased accuracy of calculated lift levels [33].

5.3 Aeroelastic simulations

Besides the field validation and the detailed experimental validation of the flap, all test activities were accompanied by aerodynamic or aeroelastic simulations. For the different phases of testing, so-called one-2-one (o2o) simulations were performed. This type of simulations are set up such that for every 10-minute measurement point, there is a corresponding 10-minute aeroelastic simulation reflecting to the extent possible the same atmospheric conditions. The measurements and simulations can then be compared in a statistical manner. The basic setup of these o2o simulations is described in [26] along with the o2o results for phase 1 and 2. The o2o results for phase 4 and part of phase 3 are reported in [34].

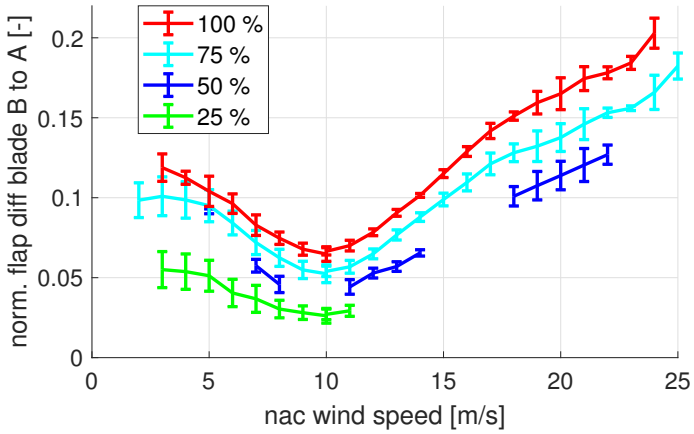

Figure 7: Relative AFS impact as function of nacelle wind speed

The focus of the aeroelastic validation is two-fold. Firstly, it serves to explore the level of accuracy of existing aeroelastic codes for validation of wind turbines with AFS (in this case SGRE's code BHawC and DTU's code HAWC2). Secondly, in combination with the b2b results and detailed aerodynamic measurements described in the previous sections, modelling gaps can be identified in order to increase the fidelity of AFS aeroelastic models. A condensed example showing the measured load control authority level of the AFS as measured on the prototype test turbine (PT) by means of b2b in comparison to the simulated levels with BHawC (BH) and HAWC2 (H2) as shown in figure 10. The figure shows a very good correlation between experiments and aeroelastic simulations, with only a slight overestimation of approximately 1% of the predictions of the aeroelastic codes in comparison with the measurements.

6 CONCLUSIONS AND LESSONS LEARNED

The Active Flap System presented in this article underwent a detailed development and validation process during the Induflap2 and VIAs projects. The main bulk of the field testing took place between 2018 and 2022. The project participants learned that the following aspects were particularly important for a successful development of the technology:

- Experimental and numerical validation work must go hand-in-hand
- Close collaboration between academia and industry is a key element
- Preliminary field validation during early design stages provides very valuable learnings for the successful development of the AFS technology.

For the AFS system developed, the main results can be summarized as follows:

- The steady state load control authority of the actuator (load handle) was measured to be between 3% and 20% depending on wind speed and actuation level of the AFS. For

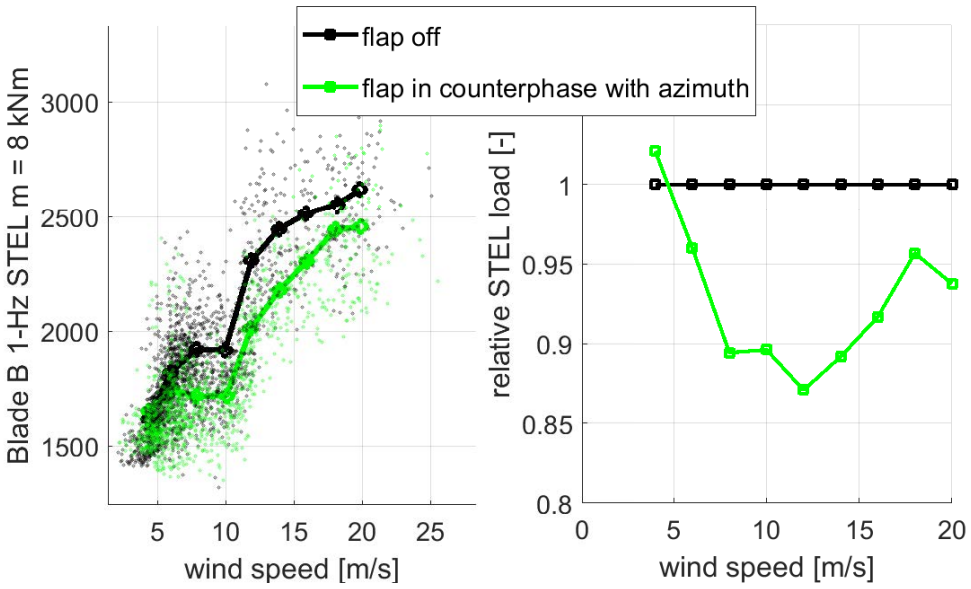

Figure 8: Impact of cyclic flap actuation of damage equivalent loads (fatigue) for a Wöhler slope of m=8 shown in absolute (left) and relative (right) level

azimuth controlled actuation, fatigue load reductions of approximately 10-13% for wind speeds around 12 m/s were measured

- Instrumentation was developed to perform detailed local aerodynamic sectional measurements based on inflow and pressure distribution measurements
- Very good agreement between aeroelastic simulations and measurements was obtained
- The b2b-method proved very beneficial in terms of measuring the load impact of the active flap at full-scale level.

To the author's knowledge, this is the largest (in terms of turbine rated power and rotor diameter) and longest (several years) field validation of an active flap ever documented, and the results collected so far are therefore an important milestone towards the development, improvement, and industrialization of the AFS. There is a need for new technologies to enable future blade designs, and although the active flap technology has not reached yet its full maturity stage, it does have future potential.

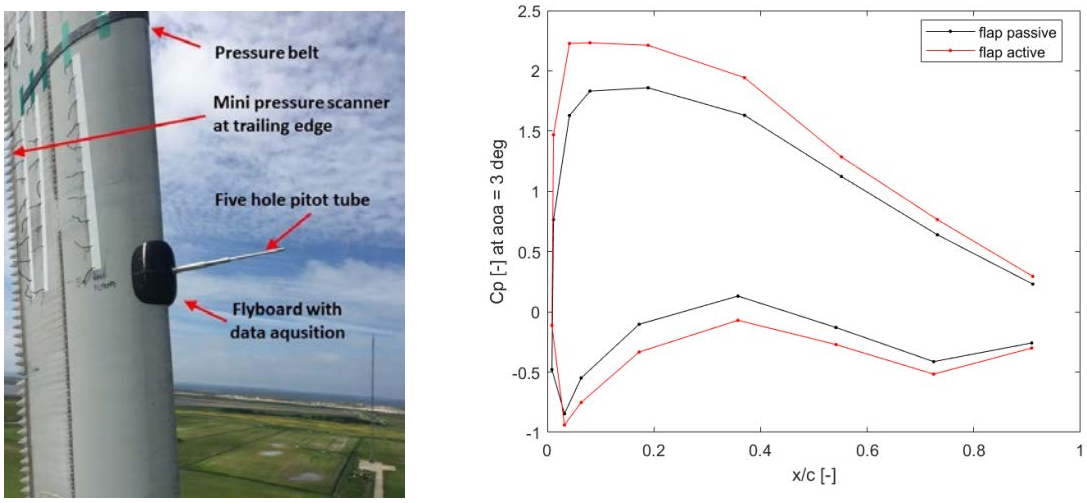

(a) Flyboard setup (b) Exemplary pressure distribution obtained from pressure belt

Figure 9: Flyboard setup including inflow sensor and pressure belt (reproduced from [32])

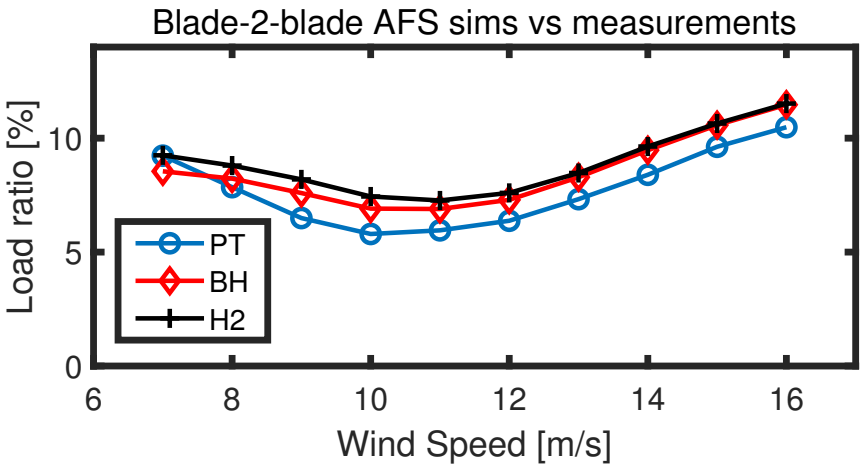

Figure 10: Blade-2-Blade from aeroelastic simulations (reproduced from [34]). Measurements from the prototype turbine are labelled with PT, and the corresponding BHawC and HAWC2 simulations with BH and H2, respectively.

REFERENCES

[1] G. Pechlivanoglou, "Passive and active flow control solutions for wind turbine blades," Ph.D. dissertation, Technische Universität Berlin, 2013.

[2] T. Barlas and G. van Kuik, "Review of state of the art in smart rotor control research for wind turbines," *Progress in Aerospace Sciences*, vol. 46, pp. 1–27, 2010.

[3] G. Pechlivanoglou, C. N. Nayeri, and C. O. Paschereit, "Performance optimization of wind turbine rotors with active flow control," *Proceedings of the ASME Turbo Expo*, vol. 1, pp. 763–775, 2011.

[4] Z. Akhter and F. K. Omar, "Review of Flow Control Devices for Wind Turbine Performance Enhancement," *Energies*, vol. 14, pp. 1–38, 2021.

[5] J. A. Meijerink and H. W. Hoeijmakersy, "Plasma actuators for active flow control on wind turbine blades," *29th AIAA Applied Aerodynamics Conference 2011*, no. June, 2011.

[6] H. Matsuda, M. Tanaka, T. Osako, K. Yamazaki, N. Shimura, M. Asayama, and Y. Oryu, "Plasma actuation effect on a MW class wind turbine," *International Journal of Gas Turbine, Propulsion and Power Systems*, vol. 9, no. 1, pp. 47–52, 2017.

[7] P. Scholz, J. Ortmanns, C. J. Kähler, and R. Radespiel, "Leading edge separation control by means of pulsed jet actuators," *Collection of Technical Papers - 3rd AIAA Flow Control Conference*, vol. 1, no. June, pp. 147–158, 2006.

[8] S. Shun and N. A. Ahmed, "Wind turbine performance improvements using active flow control techniques," *Procedia Engineering*, vol. 49, no. mm, pp. 83–91, 2012.

[9] G. Godard and M. Stanislas, "Control of a decelerating boundary layer. Part 3: Optimization of round jets vortex generators," *Aerospace Science and Technology*, vol. 10, no. 6, pp. 455–464, 2006.

[10] A. G. Oliver, "Air jet vortex generators for wind turbines," Ph.D. dissertation, City University London, 1997.

[11] V. Maldonado, "Active flow control of wind turbine blades," in *Wind turbines - design, control and applications*. Intech, 2016, ch. 13, pp. 303–324.

[12] D. J. Heathcote and D. J. Heathcote, "Aerodynamic Loads Alleviation Using Mini-tabs," Doctoral thesis, University of Bath, 2017.

[13] C. P. Van Dam, R. Chow, J. R. Zayas, and D. E. Berg, "Computational Investigations of Small Deploying Tabs and Flaps for Aerodynamic Load Control," *Journal of Physics: Conference Series*, vol. 75, pp. 1–10, 2007.

[14] P. H. Jensen, T. Chaviaropolos, and A. Natarajan, "LCOE reduction for the next generation offshore wind turbines: Outcomes from the INNWIND.EU project," *Innwind.eu*, no. October, 2017.

[15] J. Berg, M. Barone, and N. Yoder, "Smart wind turbine rotor: data analysis and conclusions," Sandia National Laboratories, Wind Energy Technologies Department, Tech. Rep. SAND2014-0712, 2014.

[16] J. Berg, B. Resor, J. Paquette, and J. White, "Smart wind turbine rotor: design and field test," Sandia National Laboratories, Wind Energy Technologies Department, Tech. Rep. SAND2014-0681, 2014.

[17] D. Castaignet, I. Couchman, N. Poulsen, T. Buhl, and J. Wedel-Heinen, "Frequency weighted model predictive control of trailing edge flaps on a wind turbine blade," *IEEE Transactions On Control Systems Technology*, vol. 21, no. 4, pp. 1105–1116, 2013.

[18] I. Couchman, D. Castaignet, N. Poulsen, T. Buhl, J. Wedel-Heinen, and N. Olesen, "Active load reduction by means of trailing edge flaps on a wind turbine blade," in *American Control Conference*, Portland, USA, June 2014.

[19] D. Castaignet, T. Barlas, T. Buhl, N. Poulsen, J. Wedel-Heinen, N. Olesen, C. Bak, and T. Kim, "Full-scale test of trailing edge flaps on a vestas v27 wind turbine: active load reduction and system identification," *Journal of Wind Energy*, 2013.

[20] D. Castaignet, J. Wedel-Heinen, T. Kim, T. Buhl, and N. Poulsen, "Results from the first full scale wind turbine equipped with trailing edge flaps," in *Proceedings of the 28th AIAA Applied Aerodynamics Conference*, 2010.

[21] "Induflap2 project website," http://www.induflap.dk, accessed 12.04.2023.

[22] H. A. Madsen, T. Barlas, and T. L. Andersen, "A Morphing Trailing Edge Flap System for Wind," *7th ECCOMAS Thematic Conference on Smart Structures and Materials*, pp. 1–10, 2015.

[23] H. A. Madsen, T. K. Barlas, and T. L. Andersen, "Testing of a new morphing trailing edge flap system on a novel outdoor rotating test rig," *European Wind Energy Association Annual Conference and Exhibition 2015, EWEA 2015 - Scientific Proceedings*, pp. 26–30, 2015.

[24] T. K. Barlas, A. S. Olsen, H. A. Madsen, T. L. Andersen, Q. Ai, and P. M. Weaver, "Aerodynamic and load control performance testing of a morphing trailing edge flap system on an outdoor rotating test rig," *Journal of Physics: Conference Series*, 2018.

[25] J. Frederik, S. Navalkar, J. W. van Wingerden, T. Barlas, H. A. Madsen, A. S. Olsen, T. L. Andersen, L. Lars, V. Riziotis, Q. Ai, P. Weaver, L. Bergami, and J. Kloepfer, "Demonstration and validation of new control concepts by dedicated and scaled turbine experiments," Innwind.eu, EU report, 2017.

[26] A. Gomez Gonzalez, T. Barlas, P. Enevoldsen, and H. Madsen, "Field test of an active flap system on a multi mw wind turbine," in *Presentations of Wind Energy Science Conference WESC2019*, Cork, Ireland, June 2019.

[27] A. Gomez Gonzalez, P. Enevoldsen, T. Barlas, H. Madsen, and A. Olsen, "Consolidated results of the laboratory and full scale field validation of an active flap system," *J. Phys.: Conf. Ser.*, 2020.

[28] A. G. Gonzalez, P. Enevoldsen, T. Barlas, and H. A. Madsen, "Test of an active flap system on a 4.3 mw wind turbine," *Journal of Physics: Conference Series*, vol. 2265, no. 3, p. 032016, may 2022. [Online]. Available: https://dx.doi.org/10.1088/1742-6596/2265/3/032016

[29] T. J. Larsen and A. M. Hansen, *How 2 hawc2, the users manual*, DTU Wind Energy.

[30] R. R. and J. Petersen, "Monopile as part of aeroelastic wind turbine simulation code," in *Proceedings of Copenhagen Offshore Wind*, 2005.

[31] P. Skjoldan, "Aeroelastic modal dynamics of wind turbines including anisotropic effects," Ph.D. dissertation, DTU, 2011.

[32] H. A. Madsen, T. K. Barlas, A. Fischer, A. S. Olsen, and A. G. González, "Inflow and pressure measurements on a full scale turbine with a pressure belt and a five hole pitot tube," *Journal of Physics: Conference Series*, vol. 2265, 2022.

[33] "Wake rake test announcement," https://www.linkedin.com/posts/helge-aagaard-madsen-ba006b93_demonstration-of-an-autonomous-measurement-ugcPost-6970317709028773888-ZeQ2?utm_source=share&utm_medium=member_desktop, accessed 12.04.2023.

[34] A. Gamberini, A. G. Gonzalez, and T. Barlas, "Aeroelastic model validation of an active trailing edge flap system tested on a 4.3 mw wind turbine," *Journal of Physics: Conference Series*, vol. 2265, no. 3, p. 032014, may 2022. [Online]. Available: https://dx.doi.org/10.1088/1742-6596/2265/3/032014